Green Chemistry

PAPER

View Article Online
View Journal | View Issue

Cite this: *Green Chem.*, 2021, **23**, 2049

Blue-light-promoted radical C–H azolation of cyclic nitrones enabled by Selectfluor®†

Alexey A. Akulov, [a] Mikhail V. Varaksin, *[a,b] Anton N. Tsmokalyuk,[a] Valery N. Charushin[a,b] and Oleg N. Chupakhin *[a,b]

Received 16th January 2021,
Accepted 3rd February 2021

DOI: 10.1039/d1gc00175b

rsc.li/greenchem

An original approach to achieve the C(sp^2)–H azolation of cyclic aldonitrones mediated by Selectfluor® has first been employed. By exploiting a metal-free, visible-light-promoted cross-dehydrogenative C–N coupling reaction between model aldonitrones, 2*H*-imidazole 1-oxides, and NH-containing azoles, a series of novel azaheterocyclic derivatives have been obtained in yields up to 94%. The elaborated protocol has proved to be appropriate for gram-scale processes and displayed potential for utilization in the synthesis of novel structural analogues of lanabecestat. Besides, mechanistic studies have revealed that this coupling reaction is likely to proceed *via* a nitroxide-involving radical pathway, encompassing a chain of electron transfer events, such as hydrogen atom transfer (HAT) and single electron transfer (SET).

Introduction

During the last decades, the family of cyclic nitrones have proved themselves to be highly valuable species not only in terms of their remarkable spin-trapping properties and therapeutic applications[1] but also due to their great synthetic potential.[2] Notably, the direct functionalization of the C(sp^2)–H bond[3] in cyclic aldonitrones is considered to be one of the most attractive approaches for their structural modification, affording novel azaheterocyclic derivatives in a step-economical manner.

Our research group has earlier reported a diverse reactivity of the C(sp^2)–H bond in model aldonitrones, 2*H*-imidazole 1-oxides, towards both electrophilic and nucleophilic reactants.[4] Most of these transformations have been found to result in the formation of new C–C bonds; however, we have recently disclosed that the use of palladium(II) catalysis in the reaction of 2*H*-imidazole 1-oxide **A** (Scheme 1a) with certain NH-azoles **B** leads to the C(sp^2)–N cross-coupling product **C**.[4c] Attempts to optimize this process by using transition metal catalysis did not give the expected results neither in demonstrating a general character of the method used nor in yields of the products. Nevertheless, we have ultimately managed to discover a facile and green-chemistry-oriented method, inspired by some seminal works reported lately.

One of such works was published in 2018 by He and co-workers, documenting the successful metal-free oxidative coupling of azines with NH-azoles mediated by Selectfluor® (Scheme 1b).[5] Widely known as an efficient and benign fluorinating agent,[6,7] Selectfluor® has also been used as an oxidant for a variety of transformations assisted by transition metals;[8] however, there has been a lack of examples of its self-sustained mediation in non-fluorinative C–H functionalization processes.[9] Later, in 2019, several impactful works were published by the Lei and Jin groups,[10] stating that Selectfluor® could be activated through irradiation with visible light. Once this happens, the active radical species thus formed are capable of inducing, for instance, the Minisci-type alkylation of azines (but not their *N*-oxides![10a]) (Scheme 1c).

We analyzed the above-mentioned publications and concluded that some chemical features described therein could be merged for achieving our objective. As a result, in this paper we wish to report the first successful examples of the Selectfluor®-mediated C(sp^2)–H azolation of cyclic nitrones promoted by visible light irradiation (Scheme 1d).

Results and discussion

As a starting point, we tried to carry out a reaction between 2*H*-imidazole 1-oxide **1a** and benzotriazole **2a**, exploiting the conditions analogous to those used in the He's work[5] with respect to azine derivatives (Table 1, entry 1). To our delight, the desired C–N coupling product **3aa** was isolated in 30% yield. Upon varying the parameters of these conditions, we found

[a]*Department of Organic & Biomolecular Chemistry, Ural Federal University, 19 Mira Str., 620002 Ekaterinburg, Russia. E-mail: chupakhin@ios.uran.ru, m.v.varaksin@urfu.ru*

[b]*Postovsky Institute of Organic Synthesis, Ural Branch of the Russian Academy of Sciences, 22 S. Kovalevskaya Str., 620990 Ekaterinburg, Russia*

†Electronic supplementary information (ESI) available. CCDC 2008292. For ESI and crystallographic data in CIF or other electronic format see DOI: 10.1039/d1gc00175b

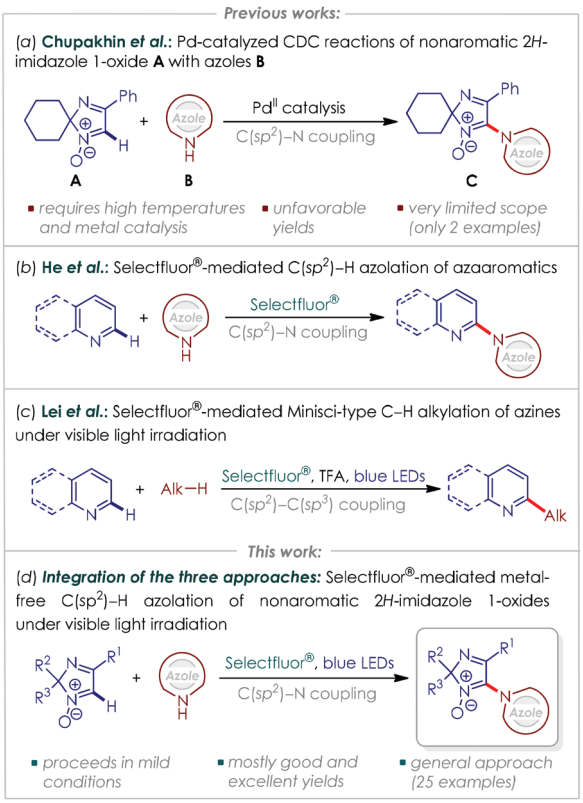

Scheme 1 Overview of the relevant previous studies and the present work.

Table 1 Initial screening of the reaction conditions[a]

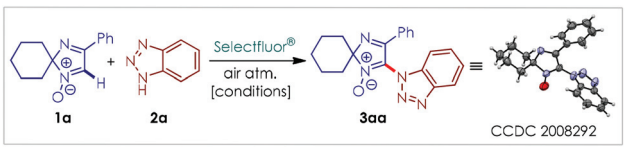

Entry	Equiv. ratio of **1a**/**2a**	Equiv. of S.F.[b]	Solvent	*t*, °C	Stirring time, h	Yield of **3aa**,[c] %
1	1.0 : 1.5	1.3	MeCN	rt	6	45 (30[d])
2	1.0 : 1.5	2.0	MeCN	rt	6	43
3	1.0 : 1.5	1.3	MeCN	70	6	60
4	1.0 : 1.0	1.3	MeCN	70	6	57
5	1.5 : 1.0	1.3	MeCN	70	6	91
6	1.5 : 1.0	1.3	MeCN	45	8	33
7[e]	1.0 : 1.5	1.3	MeCN	rt	6	47
8	1.0 : 1.5	1.3	$MeNO_2$	70	5	95
9	1.5 : 1.0	1.3	$MeNO_2$	rt	4	26
10	1.1 : 1.0	1.1	$MeNO_2$	70	4	85
11	1.5 : 1.0	1.3	MeCN/H_2O (2 : 1)	70	6	67

[a] All reactions were performed on a 0.5 mmol scale in 4.0 mL of the solvent under ambient light (unless otherwise noted). [b] S.F. = Selectfluor®. [c] Unless otherwise noted, the yield of **3aa** was determined by ^{1}H NMR spectroscopy using 1,3,5-trimethoxybenzene as an internal standard. [d] Isolated yield. [e] The experiment was carried out in darkness.

that the yields tend to increase significantly upon heating the reaction mixture (Table 1). Alterations in the nature of solvents and the molar ratio of the starting materials also proved to be

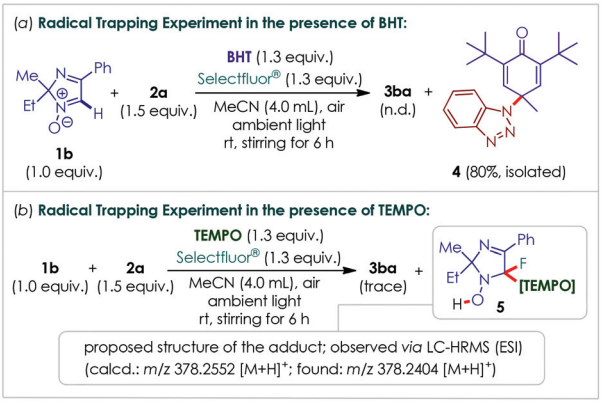

Scheme 2 Radical trapping experiments (performed on a 0.5 mmol scale).

rather substantial factors. For example, when acetonitrile was used as a solvent, the optimal ratio of **1a** and **2a** was 1.5 : 1.0 (see entry 5). In contrast, the reaction in nitromethane proceeded more efficiently with an excess of **2a** (entry 8). It should also be noted that although nitromethane seems to be appropriate for this specific transformation, it has not become the solvent of the first choice because of its hazardousness[11] and worse productivity regarding other azoles, compared with the results of analogous reactions in acetonitrile. At the same time, we could not be satisfied with the "acetonitrilic conditions" because of the poor yields of the products derived from the reaction of **1a** with azoles other than benzotriazole.

In order to define the optimal combination of the reaction parameters, we tried to gain insight into the mechanism of the process and performed some experiments in the presence of radical scavengers. In the case of the transformation studied, butylated hydroxytoluene (BHT) appears to be preferable as a radical trap rather than (2,2,6,6-tetramethylpiperidin-1-yl)oxyl (TEMPO), because the latter is known to undergo rapid oxidation by Selectfluor®, thus giving a "false positive" radical inhibition probe.[12] Nonetheless, an experiment with TEMPO has been carried out as an additional one, since TEMPO has been shown to be still capable of generating adducts with the radical species, even though Selectfluor® is present in the reaction media.[13]

In both control experiments, we observed nearly complete inhibition of the reaction of nitrone **1b** (the close analogue of **1a**) with benzotriazole **2a** (Scheme 2). Furthermore, the qualitative analysis of the reaction mixtures by LC-HRMS with electrospray ionization (ESI) clearly indicated the formation of a BHT–benzotriazole adduct,‡ thus suggesting that the coupling of **1a–b** with **2a** is likely to proceed *via* a radical pathway. The isolation and spectral characterization of the adduct allowed us to define the structure of **4** (Scheme 2a), which differed from the related adduct framework described previously by the Lei group.[14] Besides, the HRMS study afforded to presume that

‡ See ESI† for more experimental details.

the generation of the nitrone–TEMPO adduct **5** (Scheme 2b) from the corresponding radical intermediate could also take place in these trapping experiments (it is corroborated with the fact that the mass peak referring to **5** was not observed in the blank test without compounds **1b** and **2a**).

Based on the results obtained, we assumed that the interaction of **1a–b** and **2a** could be initiated by an electron transfer (ET) event between Selectfluor® and one of the reactants. Moreover, it was supposed that the productivity of the investigated coupling reaction could be enhanced if the ET process was expedited. To verify this, we decided to employ blue light irradiation as an additional driving force, since this light has been shown to facilitate the Selectfluor® homolytic cleavage,[10a] as well as to enable higher yields of the products to be achieved in comparison with analogous non-photoactivated reactions.[15] Finally, this idea proved to be a viable one (Table 2): the use of blue LEDs (λ = 440 ± 5 nm) afforded product **3aa** under mild conditions in a better yield than that derived from heating up to 70 °C (Table 2, entry 2 *vs.* Table 1, entry 5). Meanwhile, the utilization of these LEDs rather than ambient light provided nearly a three-fold increase in the yield (Table 2, entry 2 *vs.* Table 1, entry 6). In general, the re-screening of the reaction conditions allowed the most appropriate set of parameters for the further scope evaluation to be selected (Table 2, entry 2).

As the next step, we examined a series of nitrones **1a–i** and azoles **2a–q** for their compatibility with the reaction under these optimized conditions (Table 3). It has been found that the reaction demonstrates decent tolerance for functional groups; in particular, compounds bearing halogen, nitro, ethoxycarbonyl, methoxy, and trifluoromethoxy groups, as well as alkyl substituents, are appropriate for this transformation. In the case of *p*-tolyl-substituted nitrone **1e**, no side reaction at

Table 2 Re-optimization of the reaction conditions[a]

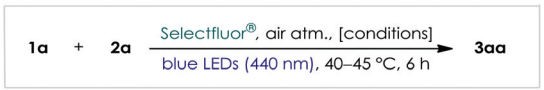

Entry	Equiv. ratio of **1a**/**2a**	Equiv. of S.F.[b]	Solvent	Yield of **3aa**,[c] %
1	1.0 : 1.0	1.3	MeCN	64
2	**1.5 : 1.0**	**1.3**	**MeCN**	**96 (84[d])**
3	1.0 : 1.5	1.3	MeCN	69
4	1.5 : 1.0	1.3	MeCN/H_2O (2 : 1)	26
5	1.5 : 1.0	NFSI, 1.3[e]	MeCN	Trace
6	1.0 : 1.0	2.0	MeCN	68
7	1.5 : 1.0	1.3	Acetone	16
8	1.5 : 1.0	—	MeCN	0

[a] For all experiments, an Aldrich® Micro photochemical reactor was used as a blue light irradiation source. All reactions were performed on a 0.5 mmol scale in 4.0 mL of the solvent at the operating temperature of the reactor (40–45 °C) (see note ‡). [b] S.F. = Selectfluor®. [c] Unless otherwise noted, the yield of **3aa** was determined *via* ^{1}H NMR spectroscopy with 1,3,5-trimethoxybenzene as an internal standard. [d] Isolated yield. [e] 1.3 equivalents of *N*-fluorobenzenesulfonimide (NFSI) were used instead of S.F.

Table 3 Reaction scope[a,b]

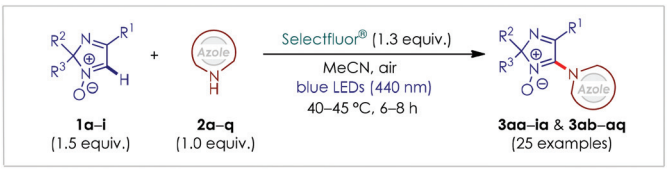

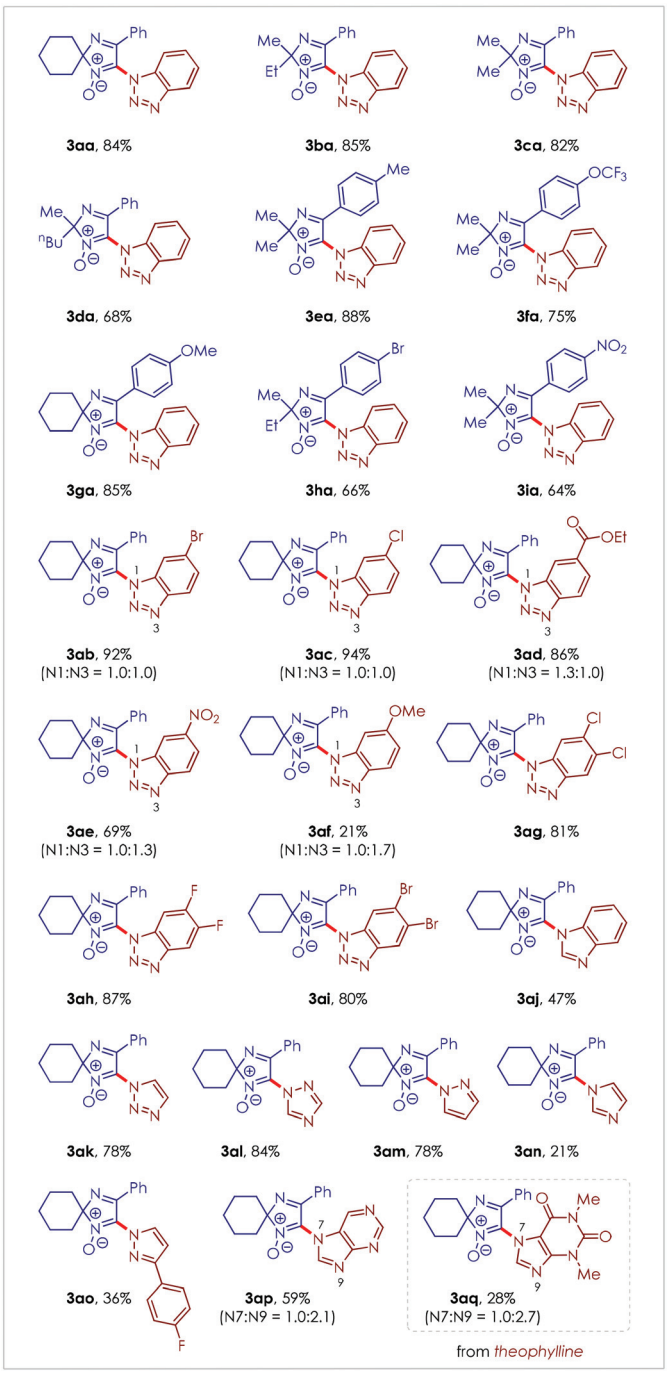

[a] Reactions were performed on a 0.5 mmol scale (unless otherwise noted in the ESI†) in MeCN (4.0 mL) under an air atmosphere using an Aldrich® Micro photochemical reactor as the blue light irradiation source (see note ‡). [b] Isolated yields are presented.

the benzylic carbon atom was observed.[16] Concerning the influence of the azole **2** scaffold, it is noteworthy that triazoles (both monocyclic and benzoannulated) provide the best results for the C–N coupling reaction (up to 94% yield). The interaction of unsubstituted 1*H*-pyrazole **2m** with **1a** gave a good result as well. Unlike this, 1*H*-imidazole **2n** reacted with **1a** to afford only 21% yield of the corresponding product **3an**. This distinction can be explained by diverse stabilities of the corresponding nitrogen-centered azolyl radicals, which are supposed to be generated during the process. In particular, the triazolyl/pyrazolyl radicals are possibly stabilized by the adjacent nitrogen lone pairs, in contrast to 1*H*-imidazolyl radical species.

An intriguing result has been obtained in the coupling reaction between **1a** and 3,5-bis(trifluoromethyl)pyrazole **2r** (Scheme 3a). Instead of the anticipated C–N coupling product **3ar**, lactam **6a** was isolated in 63% yield (relative to the starting nitrone **1a**). The behaviour of pyrazole **2r** can be explained by the enhanced steric hindrance of the nitrogen atoms, whereas compound **6a** is concluded to be derived from the corresponding oxo-containing nitroxide (*vide infra*). Besides, we also examined aromatic quinoline *N*-oxide for its reactivity in terms of the C–N coupling reaction (Scheme 3b). Unlike 2*H*-imidazole 1-oxides, quinoline *N*-oxide proved to be unreactive with azoles, thus showing a crucial role of the radical-trapping ability inherent to nitrones (which is not so typical of heteroaromatic *N*-oxides[17]).

Another point to consider was whether the reactions under study were compatible with larger loadings of the reactants. To get an answer, we carried out a gram-scale experiment with nitrone **1a** and benzotriazole **2a** (Scheme 4a). To our satisfaction, the C–N coupling product **3aa** has been obtained in 82% yield, which is comparable with that derived from small loadings. Thus, the process appears to be a scalable one, which can be regarded as an advantage for further possible applications. For instance, **3aa** and related compounds can serve as precursors towards the analogues of lanabecestat, a potent beta-secretase 1 (BACE1) inhibitor tested in the treatment of Alzheimer's disease.[18] We herein demonstrated that such analogues could be achieved *via* the deoxygenation of **3** using a RANEY® Ni – hydrazine hydrate system. Particularly, compound **8** (Scheme 4b) has been isolated in 63% yield.‡

To get a more detailed insight into the mechanism of the considered C–N coupling reaction, it was essential to clarify

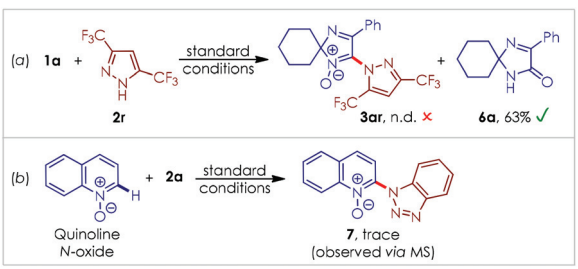

Scheme 3 Limitations of the approach.

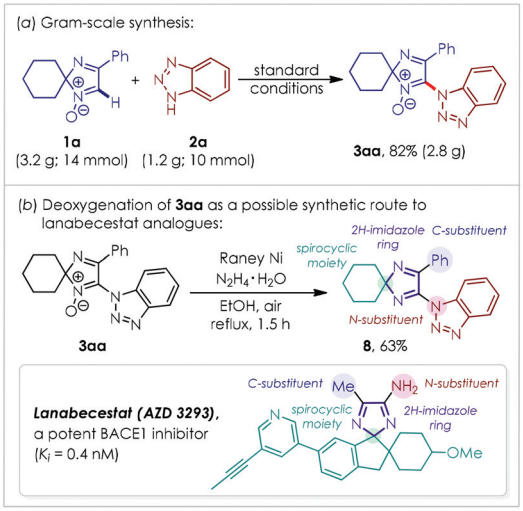

Scheme 4 Synthetic application opportunities.

how exactly blue light irradiation could activate the process. Although it has been claimed[10a] that the light induces straightforward homolytic cleavage of Selectfluor®, it still contradicts the data on the inability of this reagent to absorb the irradiation in the visible range.[19] After all, it is known that many visible-light-promoted fluorinations involving Selectfluor® are ineffective without an appropriate photosensitizer,[19b,20] thus implying that the mechanism of Selectfluor® activation has to be more sophisticated rather than the mentioned pattern of the direct light-induced N–F bond cleavage.

Initially, we supposed that the formation of a light-absorbing electron donor–acceptor (EDA) complex could take place in our case, since Selectfluor® had been shown to be capable of forming such complexes.[21] To check this hypothesis, a UV-vis spectroscopic study was performed in a manner similar to that performed by the Melchiorre group to detect EDA species.‡[22,23] However, according to the results obtained (Fig. S5, ESI†), we could not postulate the generation of any visible-light-absorbing EDA complex, since no significant bathochromic shifts for the mixtures of the reaction components have been detected. Generally speaking, one can note that the tailing of the single nitrone **1b** absorption spectrum does span over the 435–445 nm range (see Fig. S5, ESI†), yet such an absorbance level is thought to be doubtful to influence the coupling yield so dramatically, when the blue light irradiation is involved. At the same time, the Selectfluor® solution has demonstrated only trace absorbance in the visible region even at high concentrations (*i.e.* 0.1 M), thus indicating once again the unlikeliness of its direct photolysis at 440 nm.

Trying to unravel the mechanistic nature of the process, we continued our investigation by employing direct-detection electron paramagnetic resonance (DD-EPR) spectroscopy. First, the same six analytes as used for the UV-vis experiments (*i.e.* single reaction components and their binary mixtures; see Fig. S5, ESI†) were examined. The only mixture that has been found to produce stable EPR signals is the combination of

nitrone **1b** and Selectfluor® (0.1 M MeCN solution). The characterization of the obtained spectrum allowed us to assume the simultaneous involvement of two radicals, whose structures were predicted to be **R1** and **R2** (Fig. 1a), based on both previous literature data[10a,24] and our own logical inferences. The subsequent simulation of the spectrum according to the proposed structures supported this hypothesis (see Fig. 1b; note: the hyperfine coupling constants for the simulated spectrum were calculated at the B3LYP/IGLO-III level of density functional theory (DFT)). The appearance of **R2** seems to be associated with the aerobic oxidation of the **R1** derivatives (*vide infra*), explaining the origin of isolated lactam **6a** formation. Specifically, this transformation may be triggered by the Selectfluor®-derived radical dication ($TEDA^{2+\bullet}$) in a somewhat similar manner to that previously shown by Baran *et al.* for quinuclidine-promoted aerobic oxidation.[25]

An intriguing observation has been made for a single **1b** sample. Right after the dissolution of the nitrone in acetonitrile, a distinct EPR signal referred to the **1b** – OH spin adduct was detected (see Fig. S7, ESI†). As long as there was no basis for the generation of free hydroxyl radicals in the probe, it was suggested that the mentioned spin adduct could be formed by means of the Forrester–Hepburn mechanism.[26] In the case considered, this pathway implies the initial nucleophilic addition of residual water present in the solution environment to the nitrone moiety of **1b**, followed by the aerobic oxidation of thus formed hydroxylamine to the corresponding nitroxide. The detected spin adduct proved to be quite unstable though, decaying in less than 30 min (which was evidenced by its EPR signal fadeout). It should be emphasized that this adduct has not been detected when the **1b** – Selectfluor® combination is concerned, which is probably due

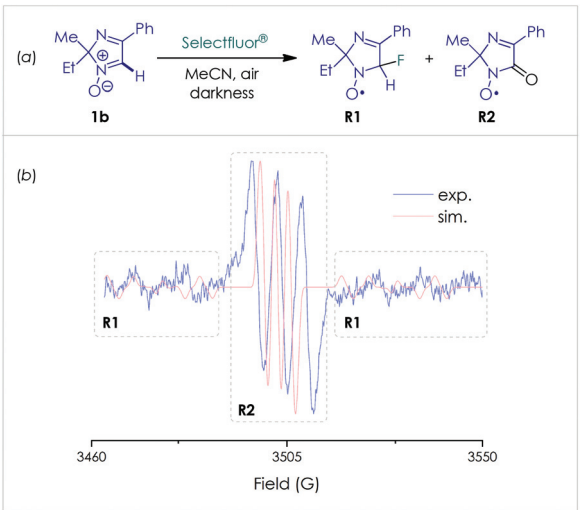

Fig. 1 (a) Proposed radicals derived from the reaction between **1b** and Selectfluor®. (b) Experimental EPR spectrum obtained for the **1b** – Selectfluor® mixture (the blue line) and the simulated EPR spectrum for the combination of **R1** and **R2** radicals (red line; the hyperfine coupling constants are calculated at the B3LYP/IGLO-III level of DFT).

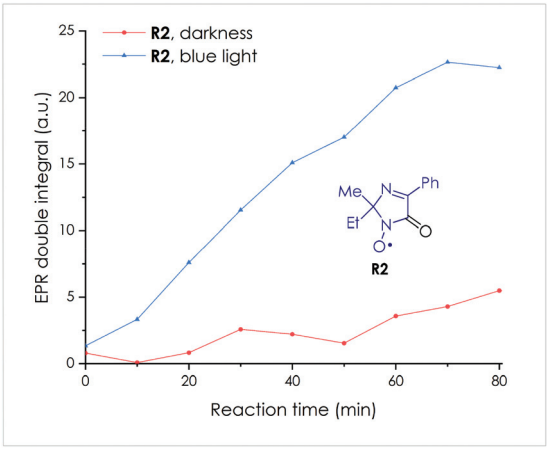

Fig. 2 Effect of blue light irradiation on the kinetics of **R2** formation.

to the immediate oxidation of its OH group to carbonyl by Selectfluor®;[27] thus the **1b** – OH spin adduct is also transformed into **R2**.

Based on the above-mentioned findings, we supposed that the Forrester–Hepburn mechanism could account for the generation of **R1** as well. In fact, the alternative inverted spin-trapping pathway[28] (*i.e.* the direct oxidation of nitrones **1** by Selectfluor®, entailing the addition of nucleophilic fluorine from the N–F reagent radical anion to the nitrone radical cation) is implausible, since the Selectfluor® oxidation potential ($E_{1/2}$ = 0.33 V *vs.* SCE[29]) is not high enough to withdraw an electron from nitrones **1** (*e.g.*, $E_{1/2}$ = 1.87 V *vs.* SCE for **1c**[30]). Along with this, the "genuine" spin-trapping pathway requires preliminary homolysis of the Selectfluor® N–F bond to release a fluorine radical, the latter being subsequently trapped by a nitrone molecule. This route is primarily unlikely for the reactions conducted in darkness, as an energy transfer source (such as light) is demanded for the bond dissociation. Meanwhile, when blue light is on, this pathway still requires an appropriate photosensitizer, since Selectfluor® itself has been shown to not absorb irradiation at 440 nm essentially; thus the N–F bond cannot be cleaved directly (in accordance with the first law of photochemistry).

We opt to verify how the rate of the radical generation would be affected by the presence of blue light. To this end, two equally concentrated **1b** – Selectfluor® solutions were analyzed by EPR spectroscopy in a time-dependent manner, one of them being examined in darkness, while the other being exposed to blue LED irradiation.‡ As anticipated, the concentration of the paramagnetic species in the irradiated sample vastly outcompeted that in the non-irradiated solution, thus supporting our previous experimental findings. This can be clearly seen in the example of **R2** progression (Fig. 2).§ When

§ Plotting analogous kinetic curves for **R1** evolution would not be reliable because of the low signal-to-noise ratio for a number of measurements and, hence, the significant error of signal double integration (however, the trend of **R1** concentration change can be assessed visually; see Fig. S8–S19, ESI†).

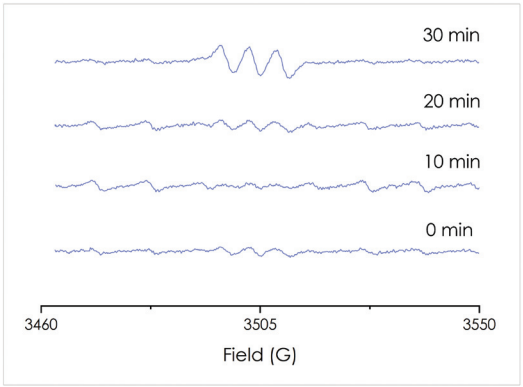

Fig. 3 EPR signal dynamics for the non-irradiated **1b** – Selectfluor® sample within the first 30 min of the reaction.

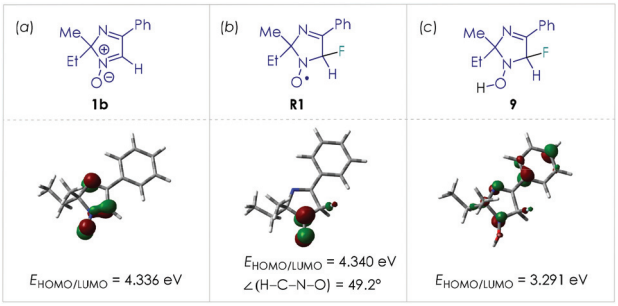

Fig. 4 HOMO electron density distributions and selected parameters for the DFT optimized structures of **1b** (a), **R1** (b), and **9** (c), calculated at the B3LYP/def2-TZVP(CH_3CN) level of theory.

the light is on, one can observe almost linear **R2** concentration growth within 1 h after mixing the components (R^2 = 0.992). In contrast, when the light is off, the kinetic character of **R2** formation is more complicated, possibly indicating a greater influence of side processes. In particular, the decrease in the concentration at the initial stage may evidence the decay of the **R2** species generated through the above-mentioned reaction of **1b** with residual water and Selectfluor® (as an oxidant) right after their dissolution in acetonitrile. The consequent accumulation of **R2** is already supposed to be dependent on the concentration of **R1**. The interconnection of **R1** and **R2** can most conveniently be noticed when considering the concerted change in their concentrations during the first 30 min of the reaction carried out in darkness (Fig. 3). Specifically, the growth of the **R2** signal intensity correlates here with the **R1** signal fadeout. Interestingly, one can remark a different picture as far as the blue-light-irradiated reaction is concerned. In this case, the **R2** signal greatly prevails over the **R1** signal throughout the entire reviewed time interval, while the latter is hardly discernible at all during the first half hour of the interaction.

These observations have prompted us to suggest that blue light tends to affect the **R1** to **R2** transition to a sufficiently greater extent than the **1b** to **R1** transformation. Hence, the actual photosensitizer may be formed *in situ* as one of the reaction intermediates. To support (or discard) this hypothesis, we have performed a series of DFT calculations, which could allow the prediction of the propensity of probable transient species to absorb irradiation in the visible range. First, we checked this predisposition with regard to nitroxide **R1** and found out the essentially equal HOMO–LUMO gap compared with that calculated for **1b** (Fig. 4a and b). Besides, the HOMO electron density distribution in an optimized model of the **R1** structure (Fig. 4b) afforded to propose a hydrogen atom transfer (HAT) to its nitroxyl moiety as the most probable pathway of its further conversion. At the same time, the alternative disproportionation of **R1** to the corresponding nitrone and hydroxylamine seems to be unfavorable in this case, as the H–C–N–O dihedral angle magnitude has been determined to be much less than the optimal one for this event 90°.[31]

To our satisfaction, when hydroxylamine **9** (Fig. 4c), being a product of the feasible HAT process, was considered for DFT characterization, the HOMO–LUMO gap for this molecule was revealed to be only 3.29 eV; that is, the absorption maximum corresponding to this electron transition turned out to be red-shifted *versus* the counterpart one for **1b** by more than 90 nm. Thus, we supposed that the absorption range of **9** would overlap the emission spectrum of the blue LEDs sufficiently enough to be responsible for the observed increase in the yields of the coupling products.

Accumulating all the obtained data, a plausible mechanism for the transformation of nitrones **1a–i** by the action of benzotriazole **2a** (as a representative example) has been proposed (Scheme 5). According to this hypothesis, nitrones **1a–i** first interact with Selectfluor®, thus producing radical dication **IM-1** and nitroxides **IM-2** (incl. **R1**). This process is presumed to occur featuring the Forrester–Hepburn mechanism; yet we cannot fully discard the probability of certain promotion at this stage in the presence of blue light given the demonstrated albeit quite weak capacity of the model nitrone **1b** to absorb irradiation in the visible range (see Fig. S5, ESI†).¶ Next, nitroxides **IM-2** are ready to accept a hydrogen atom from **2a** (HAT process) to give N-centered radicals **IM-3** and hydroxylamines **IM-4** (incl. **9**). The latter have been predicted to absorb blue light better than the starting nitrones (*vide supra*), so they are supposed to enter their excited states **IM-4***, which would be prone to donate an electron to radical dication **IM-1**[32] *via* single electron transfer (SET), thus reducing it to ammonium salt **10** and simultaneously giving radical cation **IM-5**. In darkness, the **IM-4** to **IM-5** transformation is also assumed to take place, but much more slowly indeed because of the larger energy barrier. Furthermore, the elimination of HF from **IM-4** to restore the starting nitrones may compete the aforementioned SET process. As soon as radical cations **IM-5** are formed, they can release a proton (leaving as HBF_4) to generate intermediates **IM-6**. The latter can couple with the azolyl radical **IM-3**, and the consequent HF elimination affords the

¶For instance, the overlap of only tailing of the photosensitizer absorption spectrum with the light source emission range has appeared to be enough to initiate the Selectfluor®-mediated process described in ref. 20*c*.

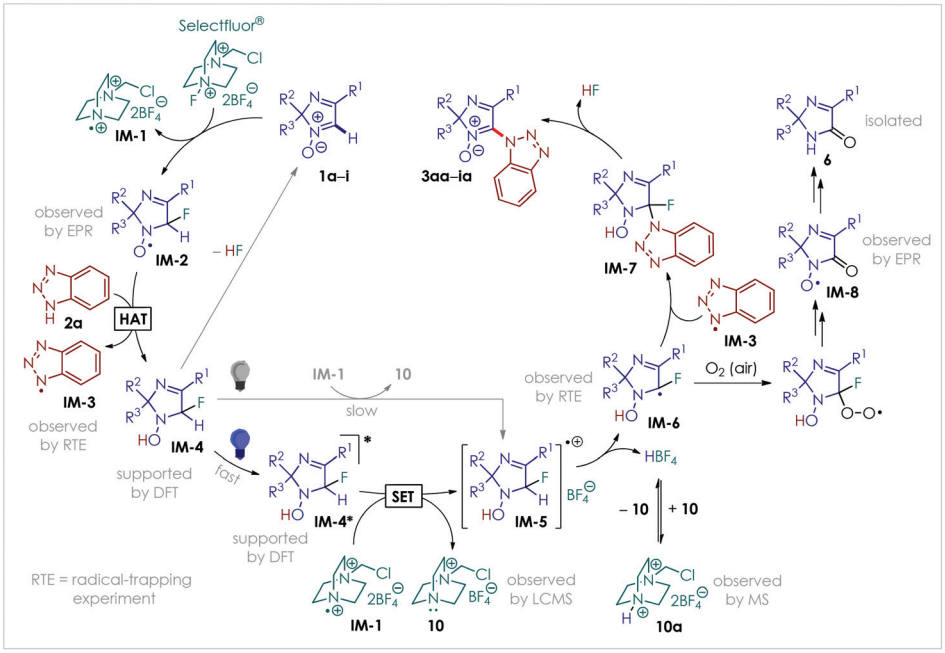

Scheme 5 Mechanistic hypothesis.

desired coupling products **3aa–ia**. Alternatively, **IM-6** can be subjected to the reaction with air oxygen, leading to nitroxides **IM-8** (incl. **R2**), the latter being eventually turned into lactams **6**.

Conclusions

In summary, we have showcased the ability of Selectfluor® to mediate the eco-friendly cross-dehydrogenative C(sp^2)–N coupling reaction of cyclic aldonitrones with NH-azoles. The mechanistic study has revealed that the process exhibits a radical nature, being essentially accelerated when the reaction mixture is exposed to blue light irradiation. Hereby, the elaborated protocol appears to be the first example of the direct *radical* C(sp^2)–H functionalization of nitrones.[2] Exploiting this approach enabled us to obtain a series of novel cyclic ketonitrone derivatives bearing azolyl substituents, which are of particular interest in terms of their potential pharmacological properties. In addition, the gram-scale experiment has shown that the reaction can be carried out with substantial loadings of starting materials, while the deoxygenation of the coupling product **3aa** has provided a potential approach towards the structural analogues of lanabecestat. Further work regarding the application of the developed approach to different heterocyclic *N*-oxides is currently underway in our laboratory.

Conflicts of interest

There are no conflicts to declare.

Acknowledgements

This research was financially supported by the Russian Science Foundation (project no. 20-43-01004).

Notes and references

1 C. Oliveira, S. Benfeito, C. Fernandes, F. Cagide, T. Silva and F. Borges, *Med. Res. Rev.*, 2018, **38**, 1159–1187.
2 S.-I. Murahashi and Y. Imada, *Chem. Rev.*, 2019, **119**, 4684–4716.
3 Selected reviews on the direct C–H bond functionalization: (*a*) A. K. Bagdi, M. Rahman, D. Bhattacherjee, G. V. Zyryanov, S. Ghosh, O. N. Chupakhin and A. Hajra, *Green Chem.*, 2020, **22**, 6632–6681; (*b*) A. A. Akulov, M. V. Varaksin, P. Mampuys, V. N. Charushin, O. N. Chupakhin and B. U. W. Maes, *Org. Biomol. Chem.*, 2021, **19**, 297–312; (*c*) Q.-Q. Kang, W. Wu, Q. Li and W.-T. Wei, *Green Chem.*, 2020, **22**, 3060–3068; (*d*) L. Capaldo, L. L. Quadri and D. Ravelli, *Green Chem.*, 2020, **22**, 3376–3396; (*e*) C.-S. Wang, P. H. Dixneuf and J.-F. Soulé, *Chem. Rev.*, 2018, **118**, 7532–7585; (*f*) J. F. Hartwig, *J. Am. Chem. Soc.*, 2016, **138**, 2–24.
4 Our previous publications concerning C(sp^2)–H functionalization of 2*H*-imidazole 1-oxides: (*a*) T. D. Moseev, M. V. Varaksin, D. A. Gorlov, V. N. Charushin and O. N. Chupakhin, *J. Org. Chem.*, 2020, **85**, 11124–11133; (*b*) A. A. Akulov, M. V. Varaksin, V. N. Charushin and O. N. Chupakhin, *ACS Omega*, 2019, **4**, 825–834; (*c*) A. A. Akulov, M. V. Varaksin, V. N. Charushin

and O. N. Chupakhin, *Chem. Heterocycl. Compd.*, 2019, **55**, 783–787; (*d*) L. A. Smyshliaeva, M. V. Varaksin, P. A. Slepukhin, O. N. Chupakhin and V. N. Charushin, *Beilstein J. Org. Chem.*, 2018, **14**, 2618–2626; (*e*) M. Varaksin, T. Moseev, O. Chupakhin, V. Charushin and B. Trofimov, *Org. Biomol. Chem.*, 2017, **15**, 8280–8284; (*f*) M. V. Varaksin, I. A. Utepova, O. N. Chupakhin and V. N. Charushin, *Tetrahedron*, 2015, **71**, 7077–7082; (*g*) M. V. Varaksin, I. A. Utepova, O. N. Chupakhin and V. N. Charushin, *J. Org. Chem.*, 2012, **77**, 9087–9093; (*h*) M. V. Varaksin, I. A. Utepova and O. N. Chupakhin, *Chem. Heterocycl. Compd.*, 2012, **48**, 1213–1219.

5 L.-Y. Xie, J. Qu, S. Peng, K.-J. Liu, Z. Wang, M.-H. Ding, Y. Wang, Z. Cao and W.-M. He, *Green Chem.*, 2018, **20**, 760–764.

6 Selected recent reports on fluorination with Selectfluor®: (*a*) M.-M. Wang and J. Waser, *Angew. Chem., Int. Ed.*, 2020, **59**, 16420–16424, (*Angew. Chem.*, 2020, **132**, 16562–16566); (*b*) J. B. Roque, Y. Kuroda, L. T. Göttemann and R. Sarpong, *Science*, 2018, **361**, 171–174; (*c*) D. S. Timofeeva, A. R. Ofial and H. Mayr, *J. Am. Chem. Soc.*, 2018, **140**, 11474–11486; (*d*) A. M. Hua, S. L. Bidwell, S. I. Baker, H. P. Hratchian and R. D. Baxter, *ACS Catal.*, 2019, **9**, 3322–3326; (*e*) E. A. Meucci, A. Ariafard, A. J. Canty, J. W. Kampf and M. S. Sanford, *J. Am. Chem. Soc.*, 2019, **141**, 13261–13267; (*f*) H. Jiang and A. Studer, *Angew. Chem., Int. Ed.*, 2018, **57**, 10707–10711, (*Angew. Chem.*, 2018, **130**, 10867–10871); (*g*) J. Sim, M. W. Campbell and G. A. Molander, *ACS Catal.*, 2019, **9**, 1558–1563; (*h*) F. J. Aguilar Troyano, F. Ballaschk, M. Jaschinski, Y. Özkaya and A. Gómez-Suárez, *Chem. – Eur. J.*, 2019, **25**, 14054–14058; (*i*) M. González-Esguevillas, J. Miró, J. L. Jeffrey and D. W. C. MacMillan, *Tetrahedron*, 2019, **75**, 4222–4227; (*j*) H. Egami, S. Masuda, Y. Kawato and Y. Hamashima, *Org. Lett.*, 2018, **20**, 1367–1370.

7 A review on Selectfluor® chemistry: P. T. Nyffeler, S. G. Durón, M. D. Burkart, S. P. Vincent and C.-H. Wong, *Angew. Chem., Int. Ed.*, 2005, **44**, 192–212, (*Angew. Chem.*, 2005, **117**, 196–217).

8 (*a*) Q. Michaudel, D. Thevenet and P. S. Baran, *J. Am. Chem. Soc.*, 2012, **134**, 2547–2550; (*b*) K. Sun, X. Wang, L. Liu, J. Sun, X. Liu, Z. Li, Z. Zhang and G. Zhang, *ACS Catal.*, 2015, **5**, 7194–7198; (*c*) J. D. Galloway, D. N. Mai and R. D. Baxter, *Org. Lett.*, 2017, **19**, 5772–5775; (*d*) Z. Wang, A. Matsumoto and K. Maruoka, *Chem. Sci.*, 2020, **11**, 12323–12328.

9 For recent advances in developing the so-called "fluorine-free" processes mediated by Selectfluor®, see: K. Yang, M. Song, A. I. M. Ali, S. M. Mudassir and H. Ge, *Chem. – Asian J.*, 2020, **15**, 729–741.

10 (*a*) L. Niu, J. Liu, X.-A. Liang, S. Wang and A. Lei, *Nat. Commun.*, 2019, **10**, 467; (*b*) X.-A. Liang, L. Niu, S. Wang, J. Liu and A. Lei, *Org. Lett.*, 2019, **21**, 2441–2444; (*c*) H. Zhao and J. Jin, *Org. Lett.*, 2019, **21**, 6179–6184.

11 D. Prat, A. Wells, J. Hayler, H. Sneddon, C. R. McElroy, S. Abou-Shehada and P. J. Dunn, *Green Chem.*, 2016, **18**, 288–296.

12 S. H. Wood, S. Etridge, A. R. Kennedy, J. M. Percy and D. J. Nelson, *Chem. – Eur. J.*, 2019, **25**, 5574–5585.

13 Y. Chen, H. Qi, N. Chen, D. Ren, J. Xu and Z. Yang, *J. Org. Chem.*, 2019, **84**, 9044–9050.

14 J. Wu, Y. Zhou, Y. Zhou, C.-W. Chiang and A. Lei, *ACS Catal.*, 2017, **7**, 8320–8323.

15 D.-M. Yan, Q.-Q. Zhao, L. Rao, J.-R. Chen and W.-J. Xiao, *Chem. – Eur. J.*, 2018, **24**, 16895–16901.

16 For a report on benzylic C–H activation using Selectfluor®, see: J. D. Galloway, D. N. Mai and R. D. Baxter, *J. Org. Chem.*, 2019, **84**, 12131–12137.

17 Nevertheless, there are studies demonstrating the possibility of radical C–H functionalization of heteroaromatic *N*-oxides, *e.g.*: (*a*) L.-Y. Xie, T.-G. Fang, J.-X. Tan, B. Zhang, Z. Cao, L.-H. Yang and W.-M. He, *Green Chem.*, 2019, **21**, 3858–3863; (*b*) L.-Y. Xie, S. Peng, F. Liu, J.-Y. Yi, M. Wang, Z. Tang, X. Xu and W.-M. He, *Adv. Synth. Catal.*, 2018, **360**, 4259–4264; (*c*) P.-T. Qin, J. Sun, F. Wang, J.-Y. Wang, H. Wang and M. Zhou, *Adv. Synth. Catal.*, 2020, **362**, 4707–4715; (*d*) D. Li, C. Liang, Z. Jiang, J. Zhang, W.-T. Zhuo, F.-Y. Zou, W.-P. Wang, G.-L. Gao and J. Song, *J. Org. Chem.*, 2020, **85**, 2733–2742; (*e*) Y.-R. Gu, X.-H. Duan, L. Yang and L.-N. Guo, *Org. Lett.*, 2017, **19**, 5908–5911; (*f*) J. P. Markham, B. Wang, E. D. Stevens, S. C. Burris and Y. Deng, *Chem. – Eur. J.*, 2019, **25**, 6638–6644.

18 N. M. Moussa-Pacha, S. M. Abdin, H. A. Omar, H. Alniss and T. H. Al-Tel, *Med. Res. Rev.*, 2020, **40**, 339–384.

19 (*a*) K. E. Danahy, J. C. Cooper and J. F. Van Humbeck, *Angew. Chem., Int. Ed.*, 2018, **57**, 5134–5138, (*Angew. Chem.*, 2018, **130**, 5228–5232); (*b*) F. Ghorbani, S. A. Harry, J. N. Capilato, C. R. Pitts, J. Joram, G. N. Peters, J. D. Tovar, I. Smajlagic, M. A. Siegler, T. Dudding and T. Lectka, *J. Am. Chem. Soc.*, 2020, **142**, 14710–14724.

20 (*a*) J.-B. Xia, C. Zhu and C. Chen, *J. Am. Chem. Soc.*, 2013, **135**, 17494–17500; (*b*) M. Rueda-Becerril, O. Mahé, M. Drouin, M. B. Majewski, J. G. West, M. O. Wolf, G. M. Sammis and J.-F. Paquin, *J. Am. Chem. Soc.*, 2014, **136**, 2637–2641; (*c*) J.-B. Xia, C. Zhu and C. Chen, *Chem. Commun.*, 2014, **50**, 11701–11704; (*d*) C. R. Pitts, B. Ling, J. A. Snyder, A. E. Bragg and T. Lectka, *J. Am. Chem. Soc.*, 2016, **138**, 6598–6609; (*e*) D. D. Bume, C. R. Pitts, F. Ghorbani, S. A. Harry, J. N. Capilato, M. A. Siegler and T. Lectka, *Chem. Sci.*, 2017, **8**, 6918–6923; (*f*) M. Xiang, Z.-K. Xin, B. Chen, C.-H. Tung and L.-Z. Wu, *Org. Lett.*, 2017, **19**, 3009–3012.

21 J.-L. Liu, Z.-F. Zhu and F. Liu, *Org. Chem. Front.*, 2019, **6**, 241–244.

22 (*a*) E. Arceo, I. D. Jurberg, A. Álvarez-Fernández and P. Melchiorre, *Nat. Chem.*, 2013, **5**, 750–756; (*b*) Z.-Y. Cao, T. Ghosh and P. Melchiorre, *Nat. Commun.*, 2018, **9**, 3274.

23 L. Buzzetti, G. E. M. Crisenza and P. Melchiorre, *Angew. Chem., Int. Ed.*, 2019, **58**, 3730–3747, (*Angew. Chem.*, 2019, **131**, 3768–3786).

24 L. Eberson and O. Persson, *J. Chem. Soc., Perkin Trans. 2*, 1997, 893–898.

25 Y. Kawamata, M. Yan, Z. Liu, D.-H. Bao, J. Chen, J. T. Starr and P. S. Baran, *J. Am. Chem. Soc.*, 2017, **139**, 7448–7451.

26 A. R. Forrester and S. P. Hepburn, *J. Chem. Soc. C*, 1971, **1971**, 701–703.
27 X. Jiang, J. Yang, F. Zhang, P. Yu, P. Yi, Y. Sun and Y. Wang, *Org. Lett.*, 2016, **18**, 3154–3157.
28 All of the spin-trapping mechanisms are clearly depicted and compared with each other here: K. Ranguelova and R. P. Mason, *Magn. Reson. Chem.*, 2011, **49**, 152–158.
29 G. P. Girina, A. A. Fainzil'berg and L. G. Feoktistov, *Russ. J. Electrochem.*, 2000, **36**, 162–163.
30 I. G. Irtegova, V. F. Starichenko, I. A. Kirilyuk and I. A. Grigor'ev, *Russ. Chem. Bull.*, 2002, **51**, 2065–2069.
31 M. Amar, S. Bar, M. A. Iron, H. Toledo, B. Tumanskii, L. J. W. Shimon, M. Botoshansky, N. Fridman and A. M. Szpilman, *Nat. Commun.*, 2015, **6**, 6070.
32 Great electron affinity of Selectfluor®-derived radical dication ($TEDA^{2+\bullet}$) has been demonstrated by the Ritter group: G. B. Boursalian, W. S. Ham, A. R. Mazzotti and T. Ritter, *Nat. Chem.*, 2016, **8**, 810–815.